

PROCEEDINGS OF SPIE

SPIDigitalLibrary.org/conference-proceedings-of-spie

X-ray measurement model and information-theoretic metric incorporating material variability with spatial and energy correlations

Ding, Yijun, Ashok, Amit

Yijun Ding, Amit Ashok, "X-ray measurement model and information-theoretic metric incorporating material variability with spatial and energy correlations," Proc. SPIE 11404, Anomaly Detection and Imaging with X-Rays (ADIX) V, 114040G (1 June 2020); doi: 10.1117/12.2557924

SPIE.

Event: SPIE Defense + Commercial Sensing, 2020, Online Only

X-ray measurement model and information-theoretic metric incorporating material variability with spatial and energy correlations

Yijun Ding ^a and Amit Ashok ^{a, b}

^a James C. Wyant College of Optical Sciences, University of Arizona, Tucson, AZ, USA;

^b Department of Electrical and Computer Engineering, University of Arizona, Tucson, AZ, USA.

ABSTRACT

Extending our prior work, we propose an X-ray measurement model that incorporates spatial-correlated material variability. The model enables more accurate task-specific assessment of the performance of X-ray imaging and sensing systems. More specifically, the model can be used to calculate bounds on the probability of error (P_e) for threat-detection tasks. We analyze the performance of a prototypical X-ray measurement system to compare the new spatial- and energy-correlated model with the previous model, which ignores the spatial correlation.

1. INTRODUCTION

Attenuation-based X-ray imaging and sensing systems are widely used for anomaly detection in security screening, medical imaging and industrial inspection. A task-specific assessment of the performance of an imaging system^{1,2} requires knowledge of the statistical properties of the forward model and the objects. The task-specific performance of X-ray systems is ultimately limited by the shot noise of the X-ray photons, and the inherent variations in the material composition.

In our prior work, we had developed a statistical multi-energy X-ray measurement model that incorporated shot noise and energy-correlated material variations.³⁻⁶ Using that measurement model, we provided analytical forms for bounds on an information-theoretic metric, the P_e .⁷ However, the inherent spatial correlations in the measurement data, which is due to the system geometry and object properties, were not considered.

In this work, we extend our prior multi-energy X-ray measurement model to incorporate both the spatial correlation and the energy correlation in the data. We then demonstrate the effects of spatial correlations on P_e bounds.

2. MEASUREMENT MODEL

A general equation to describe an X-ray transmission imaging or sensing system is:

$$\mathbf{g} = \mathcal{H}\mathbf{f} + \mathbf{n} = \mathcal{H}(\bar{\mathbf{f}} + \Delta\mathbf{f}) + \mathbf{n}, \quad (1)$$

where the data \mathbf{g} is the number of X-ray photons counted by the detector, \mathcal{H} describes the system, the object \mathbf{f} is the spatial distribution of X-ray attenuation, \mathbf{n} is the system noise, $\bar{\mathbf{f}}$ is the ensemble mean of the object, and $\Delta\mathbf{f}$ denotes the departure due to the material variability. An illustration of an X-ray measurement system is presented in Figure 1.

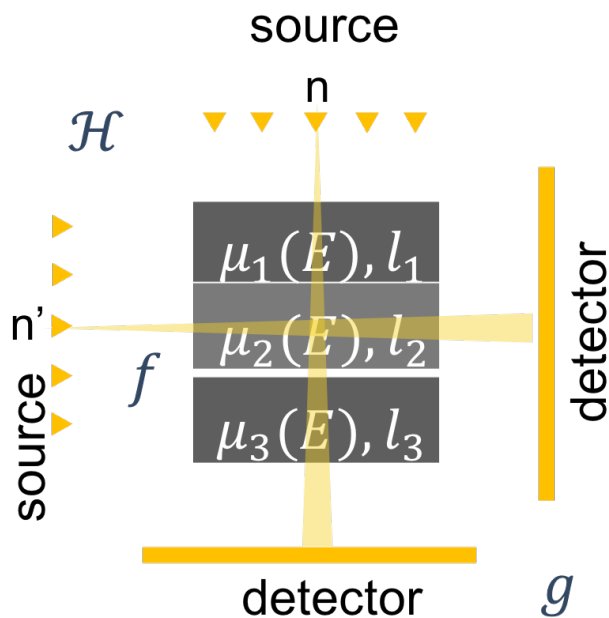


Figure 1: Illustration of an X-ray measurement system.

As presented in our previous work,³ given an object \mathbf{f} , the measurement data \mathbf{g} is a Poisson random variable

$$\text{pr}(\mathbf{g}|\mathbf{f}) = \mathcal{P}oiss(\mathbf{g}; \mathbf{J}), \quad (2)$$

where \mathbf{J} is the mean photon count for a given object and each element in \mathbf{g} is a Poisson random variable with mean equals to the corresponding element in \mathbf{J} .

The object \mathbf{f} is related to the total X-ray attenuation τ along an X-ray beam path n through the Radon transform. Each X-ray beam path penetrates multiple items, and this geometry introduces energy and spatial correlation in τ . The mean and covariance of τ is

$$\begin{aligned} \bar{\tau}_n(E) &= \sum_{t=1}^{N_{it}} \bar{\mu}_t(E) \bar{l}_{t,n}, \\ \Sigma_{\tau}(n, n', E, E') &= \sum_{t=1}^{N_{it}} \Sigma_{\tau,t}(n, n', E, E'), \end{aligned} \quad (3)$$

where the subscript n indexes the beam path, N_{it} is the number of items in the object, and $l_{t,n}$ is the path length of the item t in the X-ray path n . When each item in the object is uniformly filled with one instance of a material,

$$\Sigma_{\tau,t}(n, n', E, E') = l_{t,n} l_{t,n'} \Sigma_{\mu,t}(E, E'), \quad (4)$$

where $\Sigma_{\mu,t}(E, E')$ describes the spectral correlation of the material in item t .

When the material variation is small that the first order perturbation through Beer's law provides a good approximation, the mean photon count \mathbf{J} measured at the detector n can be expressed as:

$$\bar{\mathbf{J}}_n = N_0 \mathcal{D}S(E) e^{-\overline{\tau}_n(E)}, \quad (5)$$

where N_0 is the source photon budget, \mathcal{D} is an operator that describes the detector response, and $S(E)$ is the normalized source emission spectrum. The covariance matrix of the mean photon count \mathbf{J} is

$$\Sigma_{J,nn'} = N_0^2 \mathcal{D}[\mathbf{z}_n \mathbf{z}_{n'}^T \odot \Sigma_{\tau,nn'}] \mathcal{D}^T, \quad (6)$$

where $z_n(E) = S(E)e^{-\tau_n(E)}$ is proportional to the mean spectral photon flux that illuminates the detector.

With shot noise, the first two moments of the measurement data \mathbf{g} are

$$\bar{\mathbf{g}}_n = \bar{\mathbf{J}}_n, \quad (7)$$

and

$$\Sigma_{\mathbf{g}} = \Sigma_J + \text{diag}(\bar{\mathbf{J}}) \quad (8)$$

The expression $\text{diag}(X)$ denotes a diagonal matrix with the diagonal elements specified by the vector X .

3. ILLUSTRATIVE SYSTEM STUDY AND RESULTS

In this section, we use a prototypical X-ray bag-scanning system as an example to demonstrate the effect of spatial correlation on the performance of material-based threat detection (i.e. a binary material classification problem).

3.1 Simulation setup

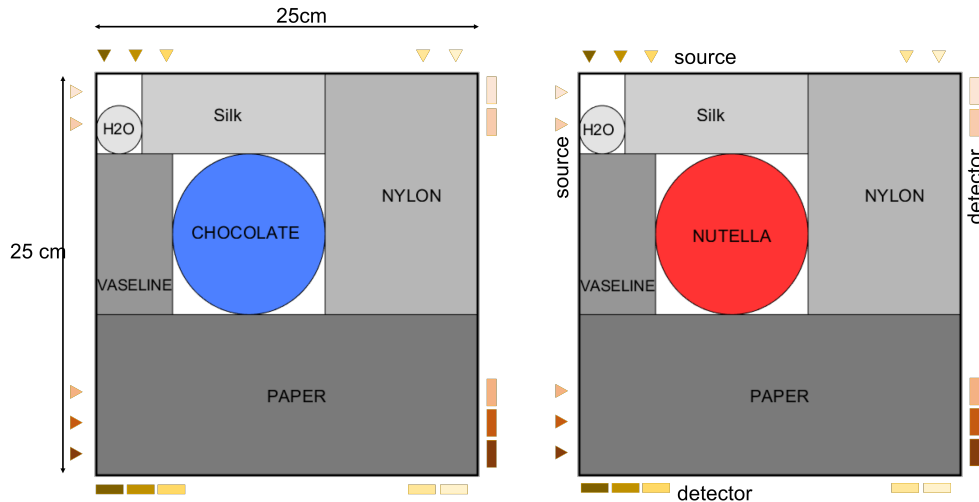


Figure 2: Simulated non-threat (left) and threat (right) bags.

The X-ray system, as illustrated in Figure 1, has 10 X-ray sources that produce pencil-beams and 10 corresponding photon-counting energy-sensitive detector elements. The 10 X-ray beam paths include five horizontal beam paths and five vertical beam paths. The X-ray sources have tungsten targets operating at 160 kVp. The corresponding source spectrum was generated with SpekCalc⁸ and has been presented in our previous work.³ The energy-sensitive detector can have one or two energy bins. The bin edges are [30, 160] keV for one bin, [30, 70, 160] keV for two bins.

An object-pair was simulated, where each object contains six items of varying sizes and varying materials. The two objects in the pair share the same geometry (aka. item shapes and materials) and are thus different by only one material. An illustration of the object pair is shown in Figure 2. We chose to use chocolate and Nutella as non-threat and threat material pair, because the attenuation properties of these two materials are similar. The same material variability library as described in our previous work,⁷ was used. Equal prevalence of the two objects were assumed for the calculation of the task-specific information-theoretic metric. The spatial correlation between data measured from different detector elements were considered when calculating the bounds on P_e . The closed form expressions of bounds on P_e were presented in our previous work.⁷

3.2 Effects of spatial correlation

We compared the spatial-correlated measurement model and spatial-uncorrelated model in terms of bounds on P_e . In the spatial-correlated model, we assumed uniform items (spatially homogeneous).

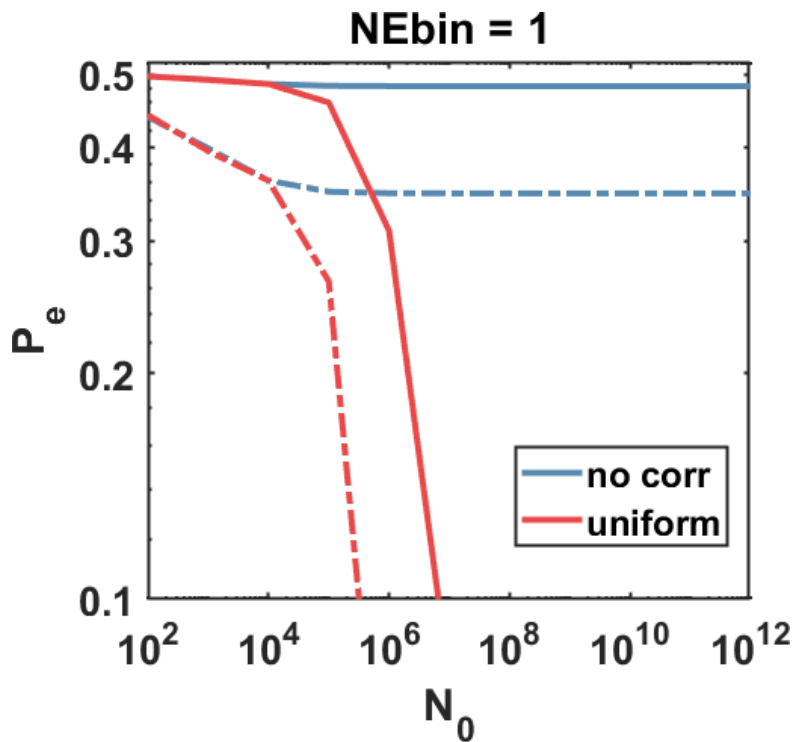


Figure 3: Bounds on P_e for the system with one energy bin, when the spatial correlation between different detector element is not considered (blue) vs. that when the items in the object are filled with uniform materials (red). Upper bounds are represented by solid line, and lower bounds are represented by dashed line.

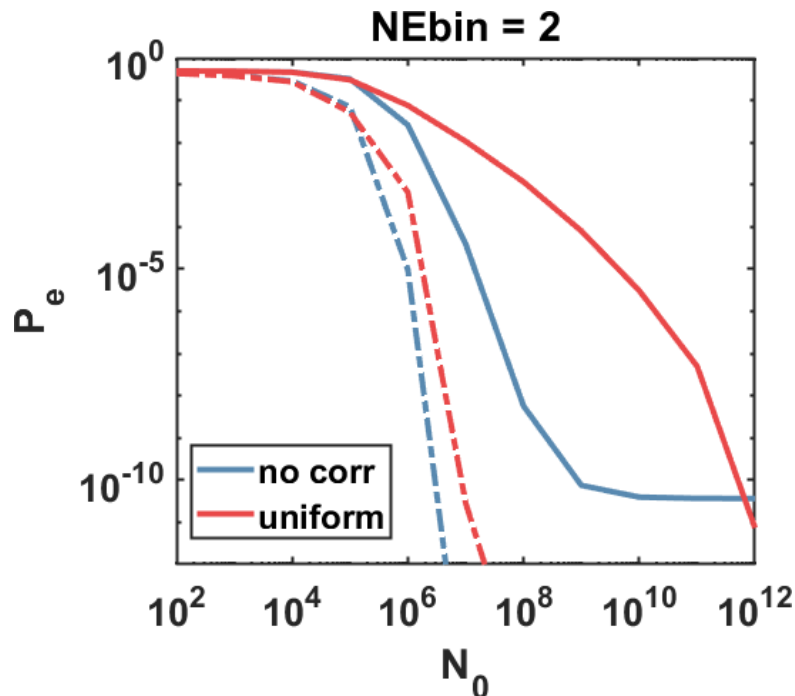


Figure 4: Bounds on P_e for the system with two energy bins, when the spatial correlation between different detector element is not considered (blue) vs. that when the items in the object are filled with uniform materials (red). Upper bounds are represented by solid line and lower bounds are represented by dashed line.

The bounds on probability of error are presented in Figure 3 for the system with one energy bin. Two models were studied, one with no spatial correlation and the other with uniform spatial correlation. When the source photon budget N_0 increases, bounds on P_e decreases and the task-specific performance improves for both models. The bounds calculated from no-spatial-correlation (NSC) model (blue) saturate at high-photon regime. This saturation is induced by the material variation. The bounds calculated from the spatial-correlated (SC) model (red) are lower than those of the no-spatial-correlation model. This agrees with our intuition, because, with one energy bin spatial correlation reduces the rank of the covariance matrix, hence the overlap between the threat and non-threat object.

Results of system with two energy bins are presented in Figure 4. For systems with two energy bins, the bounds on P_e of the SC model are looser than those of the NSC model. Compared to the NSC model, the P_e bounds of the SC model are lower at low-photon regime, higher at high-photon regime, and have the trend to be lower at ultra-high source photon budget. This shows that the relation between results of the SC model and NSC model is complex and unpredictable. Therefore, it is essential to consider spatial correlation in a realistic X-ray measurement model.

4. FUTURE WORK

To calculate the information-theoretic metric, the inverse of covariance matrix is needed. The spatial-correlated covariance matrix is prohibitively large for real systems, hence hard to invert. Our current work is focusing on developing an iterative algorithm to invert the spatial-correlated matrix for realistic systems with high dimensional measurements.

Another direction for future work is to apply this model to study the effects of the object geometry on the task performance. More specifically, the geometry of the objects includes the shape and position of the threat material and the clutter. We also plan to extend the measurement model to incorporate system uncertainties, such as fluctuations in detector quantum efficiency, variations in the source flux and the source spectrum.

5. CONCLUSION

In this work, we have presented an X-ray measurement model that considers spatial-correlated material variation and demonstrated the effects of spatial correlation on the task-specific system performance. Spatial correlation, which is intrinsic in system geometry, affects the task-specific system performance in a complex and unpredictable way. Hence, it is important to consider spatial correlation when evaluating realistic X-ray measurement systems.

6. ACKNOWLEDGEMENT

The authors gratefully acknowledge the support of the US Department of Homeland Security (DHS). The research for this project was conducted under contract with the DHS Science and Technology Directorate (S&T), contract HSHQDC-16-C-B0014. The opinions contained herein are those of the contractors and do not necessarily reflect those of DHS S&T.

REFERENCES

- [1] Neifeld, M. A., Ashok, A., and Baheti, P. K., “Task-specific information for imaging system analysis,” *JOSA A* **24**(12), B25–B41 (2007).
- [2] Barrett, H. H., “Objective assessment of image quality: effects of quantum noise and object variability,” *JOSA A* **7**(7), 1266–1278 (1990).
- [3] Ding, Y. and Ashok, A., “X-ray measurement model and information-theoretic metric incorporating material variability with energy correlations,” in [*Anomaly Detection and Imaging with X-Rays (ADIX) IV*], **10999**, 10999J, International Society for Optics and Photonics (2019).
- [4] Masoudi, A., Voris, J., Coccarelli, D., Greenberg, J., Gehm, M., and Ashok, A., “X-ray measurement model and information-theoretic system metric incorporating material variability (conference presentation),” in [*Anomaly Detection and Imaging with X-Rays (ADIX) III*], **10632**, 106320H, International Society for Optics and Photonics (2018).
- [5] Huang, J. and Ashok, A., “Information optimal compressive x-ray threat detection,” in [*Computational Optical Sensing and Imaging*], CTh2E–4, Optical Society of America (2015).
- [6] Lin, Y., Allouche, G. G., Huang, J., Ashok, A., Gong, Q., Coccarelli, D., Stoian, R.-I., and Gehm, M. E., “Information-theoretic analysis of x-ray photoabsorption based threat detection system for check-point,” in [*Anomaly Detection and Imaging with X-Rays (ADIX)*], **9847**, 98470F, International Society for Optics and Photonics (2016).
- [7] Ding, Y. and Ashok, A., “X-ray measurement model incorporating energy-correlated material variability and its application in information-theoretic system analysis,” *arXiv preprint arXiv:2002.11046* (2020).
- [8] Poludniowski, G., Landry, G., DeBlois, F., Evans, P., and Verhaegen, F., “Spekcalc: a program to calculate photon spectra from tungsten anode x-ray tubes,” *Physics in Medicine & Biology* **54**(19), N433 (2009).